In vitro multispecies Lubbock chronic wound biofilm model

Yan Sun, PhD[1]; Scot E. Dowd, PhD[1]; Ethan Smith, BSc[1]; Dan D. Rhoads, MTC[2]; Randall D. Wolcott, MD[2]

1. Medical Biofilm Research Institute, Lubbock, Texas, and
2. Southwest Regional Wound Care Center, Lubbock, Texas

Reprint requests:
Scot E. Dowd, PhD, Medical Biofilm Research Institute, 2002 Oxford Ave., Lubbock, TX 79410.
Tel: +806 789 6879;
Email: sdowd@pathogenresearch.org

Manuscript received: November 20, 2007
Accepted in final form: August 29, 2008

DOI:10.1111/j.1524-475X.2008.00434.x

ABSTRACT

Multispecies biofilms are becoming increasingly recognized as the naturally occurring state in which bacteria reside. One of the primary health issues that is now recognized to be exacerbated by biofilms are chronic, nonhealing wounds such as venous leg ulcers, diabetic foot ulcers, and pressure ulcers. Arguably three of the most important species associated with multispecies biofilms that our group sees clinically are *Pseudomonas aeruginosa*, *Enterococcus faecalis*, and *Staphylococcus aureus*. This study was conducted to address the need for a chronic pathogenic biofilm laboratory model that allows for cooperative growth of these three organisms. We have developed a novel media formulation, simple laboratory system, quantitative polymerase chain reaction for monitoring population dynamics, and methods for objectively and subjectively measuring biofilm formation. The Lubbock chronic wound pathogenic biofilm withstood treatment with a 50-fold higher concentration of bleach than that which was completely bacteriocidal for fully turbid planktonic cultures. The Lubbock chronic wound pathogenic biofilm when treated with biofilm effectors such as gallium nitrate and triclosan responded with selective inhibition of *Pseudomonas aeruginosa* or *Staphylococcus aureus*, respectively, as has been reported in the literature. The ability of this 24-hour model to react as predicted using known biofilm effectors suggests that it will lend itself to future work in the development and testing of first-generation chronic wounds pathogenic biofilm therapeutics. We have defined a realistic in vitro multispecies biofilm model simulating the functional characteristics of chronic pathogenic biofilms and developed effective tools for its characterization and analyses.

Chronic wounds affect millions of people, incur annual health care cost in the billions of dollars, and contribute in part to the mortality of hundreds of thousands of patients annually in the United States.[1–8] Typically these wounds are described by their etiology and include the general categories of diabetic foot ulcers, venous stasis ulcers, nonhealing surgical wounds, and pressure ulcers. Each of these wound types and their resistance to healing is beginning to be associated, with the presence of multispecies pathogenic microbial biofilms.[9,10] The importance of pathogenic biofilms in implants[11–16] and certain diseases[17–20] and in dentistry[21] is well documented. However, the nature and significance of chronic wound pathogenic biofilms (CWPB) as a factor in wound healing is only now beginning to be appreciated.[6,22–25] It is becoming more accepted, although it remains to be proven by the medical community, that chronic wounds are made chronic at least in part due to an unbalanced host–pathogen interaction.[9,22,26,27] This suspected imbalance, which keeps wounds chronic, is postulated to be a result of factors related to both healing (host) and also to infection (pathogenic biofilm). We are only now beginning to recognize that clinical CWPB are resistant and highly adaptable systems; we can fathom that the ability of the host to control these multispecies entities may decrease in accordance with the functional diversity of the wound's bacterial community.[28] Thus, a bacterial community that has many functionally cooperative components that are efficiently functioning to maintain the biofilm community would likely have better success in delaying healing and hindering treatments.

Although there are important multispecies models designed to model oral biofilms,[21,29] to our knowledge, there are no 24-hour in vitro multispecies biofilm models that will allow for rapid screening of therapeutics that have been able to simulate clinical CWPB. This manuscript describes the development of a media formulation, simple laboratory system, and associated methods that address the need for a 24-hour multispecies biofilm model, which possesses structural, behavioral, and functional characteristics that are similar to that of CWPB.

MATERIALS AND METHODS

Bacteria

Pseudomonas aeruginosa PAO1 (PA; ATCC number: BAA-47), *Enterococcus faecalis* V583 (EF; ATCC number: 700802), and *Staphylococcus aureus* Mu50 (SA; ATCC number: 700699) were maintained in initial cryostock cultures, resuscitated on tryptic soy agar (TSA, Sigma Chemical Co., St. Louis, MO) plates and isolated colonies were grown overnight growth in tryptic soy broth (TSB, Sigma Chemical Co.) at 37 °C with shaking at $1.0062 \times g$.

Media selection and biofilm formation detection

Microtiter polystyrene 96-well assay plates (Daigger, Vernon, IL) were used as a format to do initial screening of media formulations similar to that described by Pitts et al.[30] Bolton broth (Oxoid Ltd., Basingstock, Hampshire, UK), MRS broth (Sigma Chemical Co.), TSB, brain heart infusion (BHI; Becton, Dickinson and Company, Sparks, MD) media, and heparinized bovine plasma (Biomeda, Foster City, CA) were the final media selections (data not shown) evaluated for ability to promote overnight biofilm formation for individual inoculations containing PA, EF, or SA. Aliquots for each bacteria derived from overnight TSB were diluted and OD_{600} measured using a GENESYS-20 spectrophotometer (Thermo Scientific, Waltham, MA) and plate counts were performed using a Whitley automatic spiral plater (Don Whitley Scientific Ltd., Frederick, MD). For all studies between 1×10^3 and 1.8×10^3 CFU of each bacteria were utilized as final inoculums. For final media selection during the development process, Bolton broth, TSB, MRS, and BHI broth, containing 0, 10, 20, 30, 40, 50, or 70% plasma, were used to evaluate biofilm formation for each of the three individual bacteria. A total of 100 μL liquid media was dispensed into each microtiter well on a 96-well plate, and 1 μL of 1×10^6 CFU/mL normalized bacterial culture (10^3 bacteria) was inoculated accordingly into each well. Plates were sealed with parafilm and incubated at 37 °C with gentle shaking (.69875×*g*) for 24 hours. After incubation the media in each well was removed, transferred to a fresh plate, and the OD_{620} measured using a Bio-Rad microplate reader (Bio-Rad, Hercules, CA). The biofilm remaining in the wells was then visualized by crystal violet (CV) staining and quantified.[30] The final CV absorbance was measured using a Bio-Rad microplate reader at OD_{540}.

Lubbock chronic wound pathogenic biofilm (LCWPB) model

Bolton broth with 50% plasma and 5% freeze–thaw laked horse red blood cells (RBC) was used as the LCWPB formation media. Glass 16×150 mm test tubes with caps were autoclaved, and 6 mL biofilm formation media aseptically dispensed in each tube. Optical density-normalized cultures of the three bacteria were mixed and 10 μL of the combined and normalized culture 1×10^6 CFU/mL were inoculated into glass tubes. This inoculation was done by ejecting the pipette tip along with the bacterial suspension into the test tubes. The pipette tips act as a surface for biofilm formation in our current model. The tubes are then incubated at 37 °C within and environmental rotating incubator for 24 hours at 1.5721875×*g*.

Electron microscopy

Scanning electron microscopy (SEM) of biofilm samples was performed as follows: samples were fixed (3% paraformaldehyde and 1.5% glutaraldehyde) for 1 hour at room temperature. After dehydration in an ethanol series, the samples were transferred to hexamethyldisilazane for drying. Dried samples were mounted on aluminum stubs using aluminum paint, and sputter coated with gold. The specimens were viewed and photographed with a Hitachi S-3400N (Hitachi High Technologies, Japan) SEM. Transmission electron microscopy (TEM) was performed as follows: samples were fixed (3% paraformaldehyde and 1.5% glutaraldehyde) for 1 hour at room temperature. The samples were then processed in a Lynx microscopy tissue processor. After embedding and polymerization overnight at 60 °C, blocks were trimmed and thin sectioned to approximately 85–90 nm using a PowerTome XL ultramicrotome (Sims Co. Ltd., Seoul, Korea) and a diamond knife. The sections were collected on copper grids and stained for 15 minutes in 4% uranyl acetate and 3 minutes in lead citrate. The specimens were viewed and photographed with a Hitachi H-7650 (Hitachi) TEM.

In vivo chronic wound samples EM and visual comparison

This study was conducted in accordance with the approved Western Institutional Review Board protocol number 20062347. Subjects were invited to participate in the study upon presentation to the Southwest Regional Wound Care Center for routine wound care treatments. Written informed consent was obtained from all subjects included in the study. Chronic wounds were defined as being 30 days or older and failing to progress through normal wound healing trajectories. Subjects with chronic wounds underwent standard sharp debridements of their wounds as part of the normal course of their wound care management. The debrided material was fixed with preservative or placed in buffer, rather than being discarded as per standard protocol. For examination with SEM, tissue specimens were dehydrated with 95% ethanol. Double-sided carbon tape was used to adhere the tissue to 50 mm disk mounts. A colloidal graphite coating was used to secure the specimens and prevent charging in the SEM chamber. The mounted tissue specimens were then placed in a coating chamber and sputter coated with gold/palladium ions under a vacuum of 80 torr. The coated specimens were examined with a SEM Jeol JSM 6100 scanning electron microscope (Tokyo, Japan) using an electron beam generated by a LaB6 cathode with a voltage of 12 kV. For visual comparison of debridement and LCWPB, a venous leg ulcer was debrided using sharp debridement and placed into phosphate-buffered saline and allowed to settle naturally.

Minimal bactericidal concentration (MBC) and minimum biofilm eradicating concentration (MBEC)

A fresh 100% ultra bleach solution (containing 6% sodium hypochlorite) was used to establish MBC and MBEC for planktonic and biofilm bacteria cells. To determine the MBC, equal amounts of the three bacteria were inoculated into 5 mL TSB in glass tubes and grown at 37 °C in a shaker for 24 hours. After incubation, bleach was added directly to the tubes, making the final concentration of bleach 0.1, 0.5, 1, 2, 5, or 10%. These tubes were incubated at 37 °C with shaking (1.0062×*g*) for an additional 5 hours. After the additional incubation, 100 μL of the bleach-treated culture was plated onto a TSA plate and incubated at 37 °C overnight. The MBC was interpreted as the lowest bleach concentration to show no bacterial growth.

MBEC assays were performed in parallel with MBC determination to evaluate the lowest bleach concentration capable of eradicating biofilm cells grown using the LCWPB. To determine the MBEC, equal amounts of the three bacteria were inoculated into 5 mL of chronic wound biofilm broth in glass tubes. The biofilm cultures were prepared identically to the cultures prepared for MBC testing with the exception of the media. After incubation, bleach was added directly to the tubes, making final concentrations of bleach to 1, 5, 10, 20, 30, 40, and 50%. The tubes were subsequently incubated at 37 °C with shaking [1](120 r.p.m.) for an additional 5 hours. After subsequent incubation, the tubes were vortexed to free bacteria cells from the biofilm, and 100 μL of the bleach-treated inoculums (broth) was plated onto TSA plates and incubated at 37 °C overnight. Additionally, a piece of bleach-treated biofilm was excised from each biofilm and used to inoculate sterile glass tubes containing 5 mL TSB. These tubes were incubated at 37 °C in a shaker overnight to check the sterility of the bleach-treated biofilms. MBC and MBEC assays were all performed in triplicate.

Chemical treatment on biofilm formation

Gallium (III) nitrate hydrate (gallium) was dissolved in distilled water with sodium citrate and neutralized as described previously.[31] Triclosan (2,4,4′-trichloro-2-hydroxydiphenyl ether) was dissolved in 75% ethanol. Gallium (0.1, 1, and 10 μM) and triclosan (1, 10, and 100 p.p.m.) were tested against the LCWPB. Each treatment was evaluated comparing with control biofilms containing the respective vehicle (sodium citrate or ethanol). Individually grown bacteria cultures of EF, PA, and SA were diluted to 1×10^6 CFU/mL, and mixed together in equal amounts and were used to inoculate 5 mL of LCWPB media that contained concentrations of gallium, triclosan, or respective vehicle. The tubes were incubated at 37 °C with shaking ($1.0062\times g$) for 24 hours. Biofilm formation was subjectively observed and tubes were then vortexed for 2 minutes. The planktonic cells and biofilms were collected separately. A set of tubes were placed in an oven at 80 °C for 48 hours to obtain a dry weight. The biomass dry weight was measured as the difference of the total weight minus the empty tube weight measured before use. Tests were performed in triplicate for each treatment group. A separate set of tubes in triplicate were used for quantitative polymerase chain reaction (PCR) analyses as described below.

Primer design and reverse transcription-PCR (RT-PCR)

Genome sequences of PA (GenBank number: AE004091), EF (GenBank number: AE016830), and SA (GenBank number: BA000017) were downloaded from NCBI website. The individual genome sequence noted above were used to BLAST against each other using a WND-BLAST.[32] The selected "no-hit" genes (genes unique to each bacterium) were used to design isolate specific primers. These primers were tested for amplification efficiency and cross-reactivity. Each of the genes selected were also determined to be single copies in the respective genomes. A transcriptional regulator *LasR* gene of PA, L-ribulose-5-phosphate 4-epimerase *araD* gene of EF, and a hypothetical protein gene (Gene ID: 1120090) of SA were used to design specific primer pairs for SYBR green real-time PCR analysis by using Primer Express 2.0 (ABI, Foster City, CA). The designed primers were as follow: PA (Pseu-ae-F, 5′-TAA GGA CAG CCA GGA CTA CGA GAA-3′; Pseu-ae-R, 5′-TGG TAG ATG GAC GGT TCC CAG AAA-3′); EF (Ent-fa-F, 5′-ACC AAG CGG CGT CAA GTA TCA AGA-3′; Ent-fa-R, 5′-GTG TGC GCA ATC GCT CCA ATT TCT-3′); SA (Sta-au-F, 5′-ATT TGG TCC CAG TGG TGT GGG TAT-3′; Sta-au-R, 5′-GCT GTG ACA ATT GCC GTT TGT CGT-3′).

To test the specificity and cross-reactivity of these primers real-time PCR assays and endpoint PCR assays were performed. Genomic DNA was extracted from planktonic cells using a QIAamp DNA mini kit (Qiagen, Santa Clara, CA). DNA samples were quantified using a Nanodrop spectrophotometer (Nyxor Biotech, Paris, France). Genomic DNA from each of the three bacterial strains were diluted from 1 to 25 ng/μL per reaction and each species of DNA was individually tested against each of the other species primer sets.

Biofilm samples were ground to powder on dry ice using disposable mortar and pestles (Fisher Scientific, Waltham, MA). Bacterial genomic DNA extraction and quantification were performed as described above, and samples were diluted to a final concentration of 20 ng/μL of total DNA. The relative ratios of each bacterium were evaluated using the ABI 7500 Real Time PCR System (Applied Biosystems, Foster City, CA). Primers for PA, EF, and SA along with Bio-Rad iTaq SYBR-Green Supermix with ROX was used for 50 μL real-time quantitative PCR reactions as follows: 95 °C for 10 minutes, and 40 cycles of 95 °C for 15 seconds and 60 °C for 60 seconds. All reactions were performed in triplicate. The relative genome copy number ratios were calculated and analyzed (User Bulletin #2, ABI PRISM 7700 Sequence Detection System). In brief, the threshold cycle (C_t value) of the target genes in different samples was obtained after quantitative real-time PCR reaction. The normalizer control DNA C_t value was subtracted from the gene of interest C_t (target gene) to produce the dC_t value of the sample. The dC_t value of the calibrator (the sample with the highest dC_t value) was subtracted from every other sample to produce the ddC_t value. Two to the $-$ddC_t power ($2^{-\mathrm{dd}C_t}$) was taken for every sample and used to evaluate relative ratios of each bacteria. This real-time assay is designed to provide relative ratios of each bacterium within a given DNA extracted sample.

RESULTS AND DISCUSSION

Our goal was to develop a biofilm model that could mimic as much as possible the type of biofilm we see as part of our clinical practice. We had several criteria for this model, which included (1) multispecies model incorporating three of the bacteria typically seen together in chronic wound biofilms as part of our clinical practice; (2) synergistic growth of these three bacteria in roughly equal ratios in the biofilm; (3) biofilm formation in 24 hours allowing for a more rapid screening of biofilm effectors; (4) ability to evaluate changes in the populations of the three bacterial species; (5) ability to evaluate objectively the formation of biofilms within the model; (6) a highly visible biofilm formation to allow for rapid subjective evaluation of biofilm

formation; (7) a relatively compact and inexpensive model system (e.g., test tubes), which would allow for parallel testing of hundreds of compounds; (8) a biofilm media that utilizes three of the major host factors (damaged tissue, RBC, and plasma) that are within the wound bed; and (9) a set of tools to evaluate population dynamics (changes in the bacterial population ratios), rapid subjective visual analysis to allow for high-throughput screening, and objective quantitative measurement changes in biofilm biomass.

The model described here incorporates plasma and RBC to directly provide these components in support of our goals to better simulate the nutrient environment in a chronic wound. Additionally, the choice to utilize a chopped meat-based medium models the nutrients likely to be presented by damaged tissue in early stages after debridement. Primary tools were developed to address our goals included quantitative real-time PCR analysis to all for evaluation of population dynamics, a large highly visible biofilm biomass to allow for rapid subjective analysis of biofilm formation, and an accompanying objective analysis of biomass based on the dry weight of the biofilm. The format of the assay in test tubes allows for a rapid subjective visual evaluation of biofilm formation without the need for staining steps, while the dry weight analysis allows for an objective measurement of biomass formation.

Development of the biofilm model

A wide variety of media types were initially screened and failed to generate overnight biofilm formation for each of the isolates individually (data not shown). Ultimately, we chose several chopped meat-based media formulations as a logical foundation to simulate a chronic wound environment. Because chronic wounds can be considered rich in degraded and damaged host tissue with an abundance of extracellular matrix components. We identified chopped meat-based media as most closely resembling what nutrients are present in a wound bed. These media included Bolton broth, MRS broth, and BHI broth. TSB was also utilized as a control as it is often utilized as a biofilm-inducing media in the scientific literature. Bolton, MRS, TSB, and BHI broths with 0, 10, 20, 30, 40, 50, and 70% bovine plasma were ultimately tested for bacteria growth and overnight biofilm formation. The 96-well screening method described by Pitts et al.[30] was used to identify a media formulation that would promote biofilm formation within 24 hours for each of the three bacteria. As shown in Table 1, PA formed an obvious biofilm when growing in Bolton, TSB, or BHI broth. The strain formed more biomass with 10% plasma, but the biofilm's biomass reduced with the addition of more plasma. EF failed to form biofilm when grown in Bolton, TSB, or BHI broth alone.

Table 1. Relative CV stained results of biofilm formation on 96-well plates

	Bolton+0% plasma	Bolton+10% plasma	Bolton+25% plasma	Bolton+50% plasma	Bolton+70% plasma
Pseudomonas aeruginosa	3	3	2	++	+
Enterococcus faecalis	−−	−−	−−	6	6
Staphylococcus aureus	−−	2	3	6	6
	TSB+0% plasma	**TSB+10% plasma**	**TSB+25% plasma**	**TSB+50% plasma**	**TSB+70% plasma**
Pseudomonas aeruginosa	2	4	3	+	+
Enterococcus faecalis	−−	−−	−−	5	5
Staphylococcus aureus	−−	−−	4	5	5
	MRS+0% plasma	**MRS+10% plasma**	**MRS+25% plasma**	**MRS+50% plasma**	**MRS+70% plasma**
Pseudomonas aeruginosa	−−	1	3	3	3
Enterococcus faecalis	−−	−−	1	−−	−−
Staphylococcus aureus	−−	−−	−−	−−	−−
	BHI+0% plasma	**BHI+10% plasma**	**BHI+25% plasma**	**BHI+50% plasma**	**BHI+70% plasma**
Pseudomonas aeruginosa	2	3	2	1	1
Enterococcus faecalis	−−	−−	−−	−−	4
Staphylococcus aureus	−−	3	4	5	5

The CV absorbance was measured by using a Bio-Rad microplate reader at OD_{540}. OD_{540} readings from 0 to 0.5 were represented by ''−−,'' 0.5–1.5=''1,'' 1.5–2.5=''2,'' 2.5–3.5=''3,'' 3.5–4.5=''4,'' 4.5–5.5=''5,'' 5.5 and above=''6.'' There were three replicates analyzed for each treatment on each media array. Every media array was repeated three times. The results are averaged for replicates.

However, EF formed notable biofilm when 50% plasma concentrations were added to Bolton or TSB broth or when 70% plasma was added to BHI broth. SA formed biofilms in Bolton and BHI broth when 10% plasma was added and in TSB broth when 30% plasma was added. The amount of biomass produced by SA increased in accordance with the amount of plasma in the media. In MRS broth neither EF nor SA was able to form biofilm under any condition tested. Conversely, PA was able to form biofilm in MRS with higher concentrations of plasma. The final media for the LCWPB media was chosen and tested in a multispecies format and found to generate a 24-hour biofilm that consisted of roughly equal molar ratios of each of the three bacterial species as determined using quantitative PCR (Table 2).

The bacteria chosen for the model are those we have most often seen in chronic wound biofilms in our clinical practice and often co-occur in wounds in very similar ratios to that seen in the model.[9] Adding validation to our choice of bacteria for this model is the recent work by Gjodsbol et al.,[10] where they showed that SA, PA, and EF were the bacteria most prevalent in chronic wounds and co-occurred. They also indicated that none of the wounds were colonized by only a single bacterium, which is also what we note in our clinical practice.[9]

Examination of biofilms by electron microscopy

Although not one of the standard tools utilized as a method for evaluating biofilm formation in our model we performed SEM and TEM to evaluate the ultrastructure of the biofilm model. A complex interconnected fibrous network of EPS of differing thickness was visible when using SEM (Figure 2A), and all three types of bacterial cells were observed in the biofilm matrix (Figure 1B). The aggregation of bacterial cells within the biofilm (Figure 1C) is common in actual CWPB, and the cross-linking of the bacterial cells with the EPS (Figure 1D) is an integral part of the biofilm structure. TEM observation also showed the interconnected extracellular biofilm matrix of the LCWPB (Figure 2A). It is clear that the bacterial cells are encased in the lumen of the biofilm extracellular matrix (Figure 2B). Dividing bacterial cells were frequently observed inside the biofilm matrix (Figure 2C). Two distinct spherical types of bacterial cells were observed inside the biofilm matrix, representing the cells of EF and/or SA (Figure 2D) along with the typical rod-shaped forms of PA.

MBC and MBEC

The ability to withstand folds higher concentrations of disinfectants is a hallmark of a biofilm. To evaluate whether our biofilm had increased resistance to disinfectants, we challenged it with bleach solutions. Bleach, containing sodium hypochlorite, is widely used as an antimicrobial agent to kill bacteria, fungi, and viruses. To evaluate the LCWPB resistance to a traditional antimicrobial agent, bleach was used to compare the MBC and MBEC for planktonic and biofilm bacteria cells, respectively. For planktonic cells, which were grown overnight to concentrations of 1×10^9 CFU/mL, 1% bleach solution was required for 100% disinfection. One of the physiological characteristics of biofilms are that they should be more resistant to disinfection than planktonic cells[33]; thus, we compared MBC with MBEC. Even after 5-hour exposure to a 50% bleach solution, the LCWPB retained living cells that reproduced when inoculated onto TSA or TSB. Thus, the LCWPB exhibits at least 50-fold increased resistance to disinfection with bleach solution.

Population monitoring—RT-PCR

Here we present the development of our quantitative PCR assay, which is one of the standard tools we developed to evaluate population dynamics in the chronic wound biofilm model. In order to monitor the relative ratio of the three different species as part of the biofilm community, we developed species-specific primers with comparable

Table 2. Effect of chemical treatment on biofilm formation, dry weight, and the bacteria ratios

	Biofilm dry weight (mg ± SD)	*Paeruginosa aeruginosa*	*Enterococcus faecalis*	*Staphylococcus aureus*
Control	156.3 ± 16.5	24.7 ± 2.7%	30.5 ± 1.5%	44.7 ± 1.8%
0.1 μM gallium	122.3 ± 23.2	43.4 ± 4.8%	32.1 ± 5.3%	24.5 ± 3.5%
1 μM gallium	78.0 ± 9.8	15.0 ± 1.3%	46.8 ± 5.0%	38.3 ± 5.0%
10 μM gallium	No biofilm observed	(0.7 ± 0.1%)*	(72.9 ± 7.7%)*	(26.5 ± 5.9%)*
1 p.p.m. triclosan	108.0 ± 17.4	55.4 ± 6.7%	27.1 ± 4.5%	17.4 ± 2.8%
10 p.p.m. triclosan	66.3 ± 12.7	47.2 ± 6.7%	49.8 ± 4.9%	3.0 ± 0.1%
100 p.p.m. triclosan	42.7 ± 8.5	61.9 ± 7.3%	37.9 ± 5.9%	0.2 ± 0.0%

This table provides the objective measurement of biomass in dry weight during each of the treatments used to verify the functionality of the Lubbock chronic wound biofilm model. It also provides a normalized ratio for each of the bacteria within the biomass. It should be noted that in the control biofilm each of the three bacteria are present in nearly equal ratios. Thus, this system provides a valuable model for characterizing the differential effects of treatments on diverse populations. The dry weights were means for three replicates for each treatment. The bacteria ratios were calculated based on the C_t values of qRT-PCR. Every qRT-PCR array was repeated three times with three replicates. The results are means for nine replicates.

*These are the ratios of planktonic cells from 10 μM gallium-treated cultures included for reference only, as no visible biofilm was formed.

QRT-PCR, quantitative reverse transcription-polymerase chain reaction.

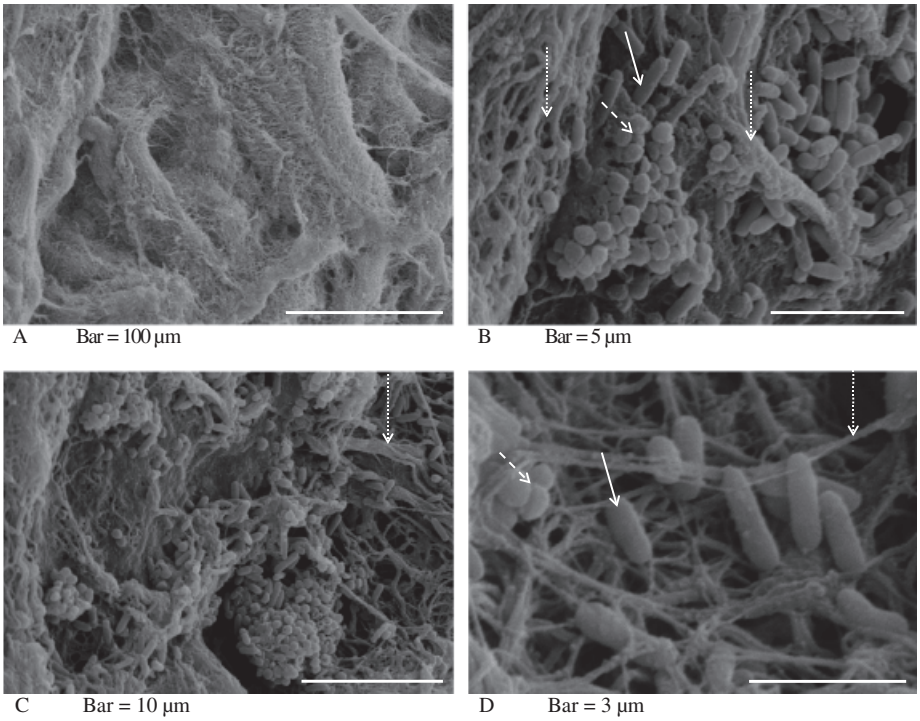

Figure 1. Scanning electron micrographs of the Lubbock chronic wound biofilm model. These micrographs illustrate the complex extracellular matrix (dotted arrows) created by the bacteria. Higher magnification images show both rod (solid arrow) and cocci bacteria (dashed arrow) in close proximity indicating the cooperative interaction of these populations.

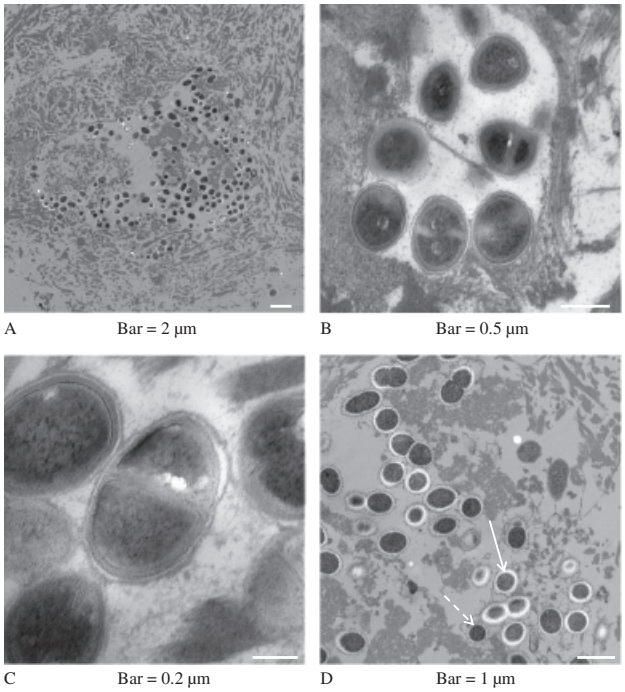

Figure 2. Transmission electron micrographs of the Lubbock chronic wound biofilm model. The transmission micrographs are able to show not only the coexistence of rod and cocci populations as seen in SEM (Figure 1), but also the cohabitation of two species of cocci. In (D) we can see *Enterococcus* with the larger halo (solid arrow) surrounding the cell and *Staphylococcus* with the compact halo (dashed arrow). These images show how the bacteria congregate in enclosed and protected foci within the biofilm.

amplification efficiencies. These primers were proven specific for each of the respective species. When relatively low concentrations (20 ng) of DNA were used for SYBR green real-time PCR analysis, the threshold cycle (C_t) values of the gene amplification were in the range of 20–22 and the background C_t values were > 33, indicating the specificity of these three primers. The C_t functions and relative ratios were also shown to be consistent and predictable when DNA from each isolate was mixed in various known ratios normalized to genome copy number. Extensive evaluation of the primers was performed to ensure their linear amplification range, proper dissociation curves, and lack of nonspecific amplification over extended cycling. Dissociation curves of all PCR products showed sharp peaks for each primer pairs at the expected T_m of the products (data not shown). Figure 3 illustrates the linear plots of the C_t value versus the DNA dilutions of these three bacteria, indicating high real-time PCR amplification efficiency along with the noted specificity. These results clearly showed that the three primer pairs were specific and sensitive within this system and able to be used to monitor the populations of each of the three species within the biofilm community.

Treatment response evaluation: exemplifying the use of the LCWPB

We wanted to perform a cursory evaluation of how the populations of bacteria in the biofilm model responded to two treatment agents we have evaluated clinically and to exemplify how this model can be used to evaluate treatment agents. The LCWPB was exposed to various concentrations of gallium or triclosan to evaluate the population responses within the biofilm community. Subjective observations of the biofilm formation were also made (Table 2)

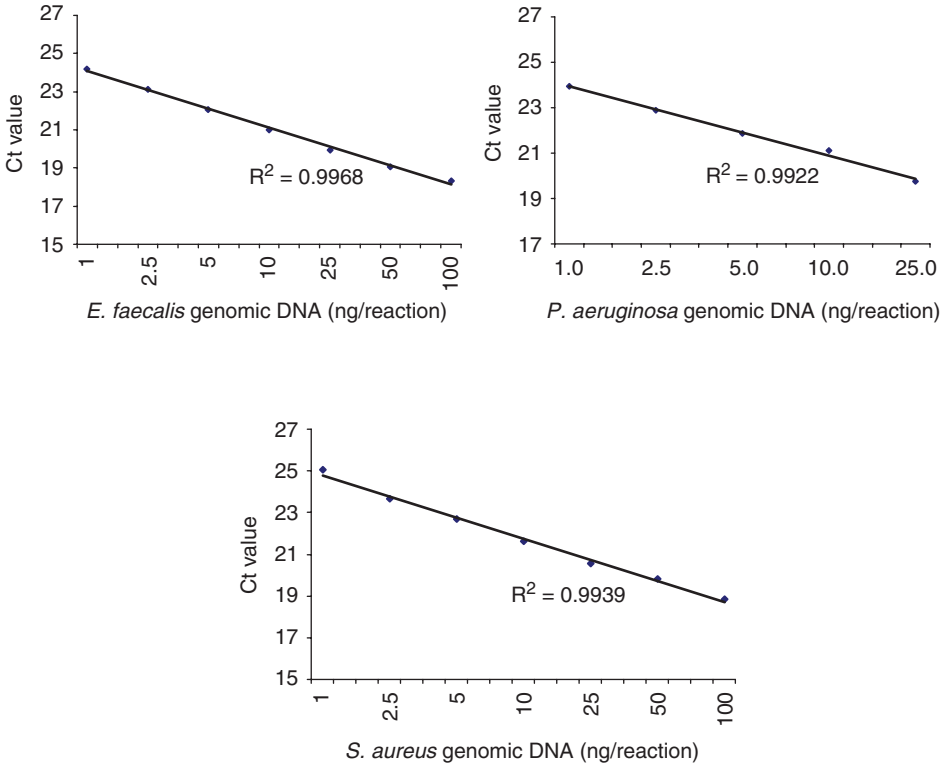

Figure 3. Linear plots of the qRT-PCR amplification profile for diluted genomic DNA. (A) *Pseudomonas aeruginosa*, (B) *Enterococcus faecalis*, and (C) *Staphylococcus aureus*. qRT-PCR, quantitative reverse transcription-polymerase chain reaction.

and the biomass dry weight was also measured, which provides objective measurement of biofilm formation. Both of the treatments, as expected, exhibited lower biomass formation, based on dry weight, than the control biofilms, and the decrease of the biomass correlated with the visible reduction of the biofilm formation (Table 2). Gallium and triclosan both demonstrated an obvious and significant ($p < 0.01$) inhibitory effect on biofilm formation. No visible biofilm was evident following treatment with 10 μM gallium and significantly ($p < 0.01$) less biofilm formed with 10 or 100 p.p.m. triclosan (Table 2). To further characterize the effects the chemicals had on the individual bacterial populations within the mixed species biofilm, the real-time PCR assay developed as part of this study was utilized. This test was used to compare vehicle-only controls with the gallium- and triclosan-treated samples. Gallium was seen to have a marked inhibition of PA ($p < 0.01$) at 1 μM over both SA and EF. Triclosan had a selective inhibitory effect on SA ($p < 0.01$) at all three concentrations (Table 2) over PA and EF. These results provide validation of the biofilm model as a system to evaluate treating agents and exemplifies the predictable response of the model and its bacterial populations to well-documented treatments.

Triclosan has been extensively studied as an antibacterial agent.[34] It is particularly noted for ability to affect *Streptococcus* and *Staphylococcus* spp.[35–37] while other studies have shown that *Pseudomonas* spp. is resistant[35,38] or even able to inactivate triclosan.[39] Our results agreed with previous findings that PA is more tolerant of triclosan than SA. In contrast to triclosan, gallium nitrate has been reported to be most effective against *Pseudomonas* spp. biofilms.[31] This is, however, likely the first report of gallium nitrate's activity against a multispecies biofilm containing SA and EF. PA was shown here to be the most sensitive of the three organisms to the inhibitory effects of gallium at the lower concentrations tested. At higher concentrations of gallium, all three bacteria showed sensitivity to the treatment.

In conclusion, one of the most encouraging aspects of this in vitro model is the morphological similarity we see with the naked eye (Figure 4) and electron micrographs (Figure 5), compared with that seen in actual chronic wound biofilms. While there are inherent artifacts generated by the preparation of such samples for EM work,[40] we still see the similarity in the component structure when comparing the LCWPB with actual CWPB. This study reveals that distinct and seemingly realistic interconnected fibrous networks of the extracellular matrix are formed within the LCWPB. During the media selection process of biofilm formation, bovine plasma was found to be critical for this kind of "wound-like" biofilm growth. Early tests with serum-based media, for instance, did not yield this type of result (data not shown). It is likely that SA coagulase enzyme and its ability to convert fibrinogen to fibrin plays a key role in developing the anatomy of the LCWPB EPS.

Taken together, the effects of these chemical treatments and the development of population and biomass measurements show the functionality of the LCWPB as a valuable in vitro method for the study of the chronic wound paradigm. Our media, which contains laked RBC, plasma, and a foundation derived from chopped meat (Bolton media), represents a logical nutritional base, which can arguably simulate the nutrients available to bacteria in a wound

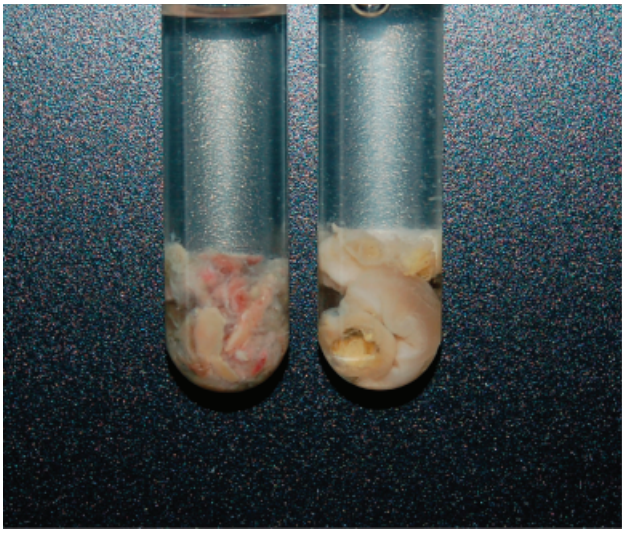

Invivo *Invitro*

Figure 4. Visual comparison of an actual debridement sample taken from chronic wound biofilm with the Lubbock chronic wound biofilm. This image compares a typical chronic wound biofilm on the left and the Lubbock chronic wound biofilm on the right showing the similarity in texture and consistency between the in vivo biofilms we typically recover and the in vitro model described in this manuscript.

environment. This model provides a functional system for future testing of additional host factors, antimicrobial, and antibiofilm treatments. The rapidity of biofilm development and maturation, the ease of use, the tools described herein for evaluation of the individual bacterial populations, a heterogeneous composition, high reproducibility, the use of plasma and RBC, and the relatively low cost of the model provides definite advantages for the study of the chronic wound biofilm paradigm. This model will facilitate the search for therapeutics that can effectively target chronic wound biofilms and other biofilm diseases and is now being used to screen next generation biofilm effectors. Current work is focused on the refinement of the model conditions, fine tuning the analytical measurement tools, development of new analytical tools (e.g., population microarrays), and increasing the functional and species diversity of the bacterial populations within the model.

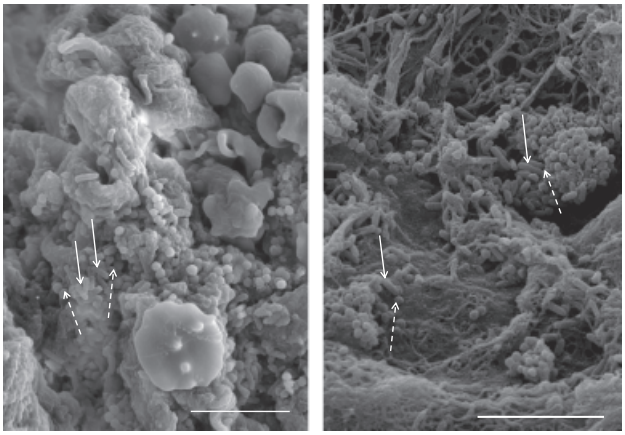

In Vivo Bar = 10 μm *In Vitro* Bar = 10 μm

Figure 5. Scanning electron micrograph comparison of in vivo and in vitro biofilms. These images, which are at only slightly different magnifications, highlight the similarity in the structure and community of the biofilm and its resident bacterial populations. In both images we can see rod-shaped (solid arrows) and cocci-shaped bacteria (dashed arrows) in close proximity.

ACKNOWLEDGMENTS

USDA disclaimer: The use of trade, firm, or corporation names in this publication is for the information and convenience of the reader. Such use does not constitute an official endorsement or approval by the United States Department of Agriculture.

REFERENCES

1. Church D, Elsayed S, Reid O, Winston B, Lindsay R. Burn wound infections. *Clin Microbiol Rev* 2006; 19: 403–34.
2. Beckrich K, Aronovitch SA. Hospital-acquired pressure ulcers: a comparison of costs in medical vs. surgical patients. *Nurs Econ* 1999; 17: 263–71.
3. Landi F, Onder G, Russo A, Bernabei R. Pressure ulcer and mortality in frail elderly people living in community. *Arch Gerontol Geriatr* 2007; 44 (Suppl. 1): 217–23.
4. Perencevich EN, Sands KE, Cosgrove SE, Guadagnoli E, Meara E, Platt R. Health and economic impact of surgical site infections diagnosed after hospital discharge. *Emerg Infect Dis* 2003; 9: 196–203.
5. Davis LE, Cook G, Costerton JW. Biofilm on ventriculoperitoneal shunt tubing as a cause of treatment failure in coccidioidal meningitis. *Emerg Infect Dis* 2002; 8: 376–9.
6. Davis SC, Martinez L, Kirsner R. The diabetic foot: the importance of biofilms and wound bed preparation. *Curr Diab Rep* 2006; 6: 439–45.
7. Ramsey SD, Newton K, Blough D, McCulloch DK, Sandhu N, Wagner EH. Patient-level estimates of the cost of complications in diabetes in a managed-care population. *Pharmacoeconomics* 1999; 16: 285–95.
8. Boyko EJ, Ahroni JH, Stensel V, Forsberg RC, Davignon DR, Smith DG. A prospective study of risk factors for diabetic foot ulcer. The Seattle Diabetic Foot Study. *Diabetes Care* 1999; 22: 1036–42.
9. James GA, Swogger E, Wolcott R, Pulcini ED, Secor P, Sestrich J, Costerton JW, Stewart PS. Biofilms in chronic wounds. *Wound Repair Regen* 2008; 16: 37–44.
10. Gjodsbol K, Christensen JJ, Karlsmark T, Jorgensen B, Klein BM, Krogfelt KA. Multiple bacterial species reside in chronic wounds: a longitudinal study. *Int Wound J* 2006; 3: 225–31.
11. Nickel JC, Heaton J, Morales A, Costerton JW. Bacterial biofilm in persistent penile prosthesis-associated infection. *J Urol* 1986; 135: 586–8.
12. Holland SP, Pulido JS, Miller D, Ellis B, Alfonso E, Scott M, Costerton JW. Biofilm and scleral buckle-associated infections. A mechanism for persistence. *Ophthalmology* 1991; 98: 933–8.

13. Ward KH, Olson ME, Lam K, Costerton JW. Mechanism of persistent infection associated with peritoneal implants. *J Med Microbiol* 1992; 36: 406–13.
14. Costerton JW. Biofilm theory can guide the treatment of device-related orthopaedic infections. *Clin Orthop Relat Res* 2005; 437: 7–11.
15. Crump JA, Collignon PJ. Intravascular catheter-associated infections. *Eur J Clin Microbiol Infect Dis* 2000; 19: 1–8.
16. Malaisrie SC, Malekzadeh S, Biedlingmaier JF. In vivo analysis of bacterial biofilm formation on facial plastic bioimplants. *Laryngoscope* 1998; 108 (Part 1): 1733–8.
17. Nickel JC, Emtage J, Costerton JW. Ultrastructural microbial ecology of infection-induced urinary stones. *J Urol* 1985; 133: 622–7.
18. Costerton JW, Stewart PS, Greenberg EP. Bacterial biofilms: a common cause of persistent infections. *Science* 1999; 284: 1318–22.
19. Costerton JW. Cystic fibrosis pathogenesis and the role of biofilms in persistent infection. *Trends Microbiol* 2001; 9: 50–2.
20. Leid JG, Costerton JW, Shirtliff ME, Gilmore MS, Engelbert M. Immunology of Staphylococcal biofilm infections in the eye: new tools to study biofilm endophthalmitis. *DNA Cell Biol* 2002; 21: 405–13.
21. Bradshaw DJ, Marsh PD, Allison C, Schilling KM. Effect of oxygen, inoculum composition and flow rate on development of mixed-culture oral biofilms. *Microbiology* 1996; 142 (Part 3): 623–9.
22. Saye DE. Recurring and antimicrobial-resistant infections: considering the potential role of biofilms in clinical practice. *Ostomy Wound Manage* 2007; 53: 46–8, 50, 52.
23. Edwards R, Harding KG. Bacteria and wound healing. *Curr Opin Infect Dis* 2004; 17: 91–6.
24. White RJ, Cutting K, Kingsley A. Topical antimicrobials in the control of wound bioburden. *Ostomy Wound Manage* 2006; 52: 26–58.
25. Williams C. Wound care: askina transorbent and askina biofilm transparent. *Br J Nurs* 2000; 9: 304–7.
26. Percival SL, Bowler PG, Dolman J. Antimicrobial activity of silver-containing dressings on wound microorganisms using an in vitro biofilm model. *Int Wound J* 2007; 4: 186–91.
27. Bjarnsholt T, Kirketerp-Moller K, Jensen PO, Madsen KG, Phipps R, Krogfelt K, Hoiby N, Givskov M. Why chronic wounds will not heal: a novel hypothesis. *Wound Rep Regen* 2008; 16: 2–10.
28. Boles BR, Thoendel M, Singh PK. Self-generated diversity produces "insurance effects" in biofilm communities. *Proc Natl Acad Sci USA* 2004; 101: 16630–5.
29. Keevil CW, Bradshaw DJ, Dowsett AB, Feary TW. Microbial film formation: dental plaque deposition on acrylic tiles using continuous culture techniques. *J Appl Bacteriol* 1987; 62: 129–38.
30. Pitts B, Hamilton MA, Zelver N, Stewart PS. A microtiter-plate screening method for biofilm disinfection and removal. *J Microbiol Methods* 2003; 54: 269–76.
31. Kaneko Y, Thoendel M, Olakanmi O, Britigan BE, Singh PK. The transition metal gallium disrupts *Pseudomonas aeruginosa* iron metabolism and has antimicrobial and antibiofilm activity. *J Clin Invest* 2007; 117: 877–88.
32. Dowd SE, Zaragoza J, Rodriguez JR, Oliver MJ, Payton PR. Windows. NET network distributed basic local alignment search toolkit (W.ND-BLAST). *BMC Bioinformatics* 2005; 6: 93.
33. Donlan RM, Costerton JW. Biofilms: survival mechanisms of clinically relevant microorganisms. *Clin Microbiol Rev* 2002; 15: 167–93.
34. Bradshaw DJ, Marsh PD, Watson GK, Cummins D. The effects of triclosan and zinc citrate, alone and in combination, on a community of oral bacteria grown in vitro. *J Dent Res* 1993; 72: 25–30.
35. Jones GL, Muller CT, O'Reilly M, Stickler DJ. Effect of triclosan on the development of bacterial biofilms by urinary tract pathogens on urinary catheters. *J Antimicrob Chemother* 2006; 57: 266–72.
36. Phan TN, Marquis RE. Triclosan inhibition of membrane enzymes and glycolysis of Streptococcus mutans in suspensions and biofilms. *Can J Microbiol* 2006; 52: 977–83.
37. Steinberg D, Tal T, Friedman M. Sustained-release delivery systems of triclosan for treatment of Streptococcus mutans biofilm. *J Biomed Mater Res B Appl Biomater* 2006; 77: 282–6.
38. Moretro T, Sonerud T, Mangelrod E, Langsrud S. Evaluation of the antibacterial effect of a triclosan-containing floor used in the food industry. *J Food Prot* 2006; 69: 627–33.
39. Meade MJ, Waddell RL, Callahan TM. Soil bacteria *Pseudomonas putida* and *Alcaligenes xylosoxidans* subsp. denitrificans inactivate triclosan in liquid and solid substrates. *FEMS Microbiol Lett* 2001; 204: 45–8.
40. Reese S, Guggenheim B. A novel TEM contrasting technique for extracellular polysaccharides in in vitro biofilms. *Microsc Res Tech* 2007; 70: 816–22.